

ANALYSIS OF THERMAL VARIANCE EQUATION FOR NATURAL CONVECTION OF AIR AND SODIUM

M. Wörner and G. Grötzbach

Kernforschungszentrum Karlsruhe, Institut für Reaktorsicherheit,
Postfach 3640, D-76021 Karlsruhe, Germany

ABSTRACT

In this paper we use a direct simulation data base of turbulent Rayleigh-Bénard convection to investigate statistical features of temperature fluctuations in natural convection. Results are given for the balance of temperature variance $\overline{T'^2}/2$ for two different fluids, air and liquid sodium. They reveal that in natural convection there is no local equilibrium between production and dissipation of $\overline{T'^2}/2$, but diffusive transport of $\overline{T'^2}/2$ is of great importance. Analysis of the conventional diffusion model indicates deficiencies of the gradient diffusion concept. The ratio between kinematic and thermal time scales, which is often used to model the sink term in the $\overline{T'^2}/2$ -equation, is found to depend significantly on the Prandtl number.

KEYWORDS

Direct numerical simulation, Rayleigh-Bénard convection, temperature variance equation.

INTRODUCTION

Although available computer power is always increasing, direct solution of the Navier-Stokes and energy equation is possible only for few problems of practical interest (Grötzbach, 1994). For the calculation of turbulent flow and heat transfer in most engineering applications, only the approach by statistical turbulence models is feasible at present. The most commonly used model is the k - ϵ model, which uses an isotropic eddy viscosity and a turbulent Prandtl number to model the unknown turbulent stresses and heat fluxes (e.g. Rodi, 1980). While this concept yields satisfactory results for turbulent heat transfer for most forced flows, it is unsuitable for flows that are dominated by buoyancy forces and thus are strongly anisotropic (Peeters &

Henkes, 1992). To obtain realistic predictions of turbulent heat transfer in natural convection, models are needed which are based on the transport equation of Reynolds stresses $\overline{u_i' u_j'}$ and turbulent heat fluxes $\overline{u_i' T'}$. These equations contain several higher order correlations which can hardly be measured, but nevertheless have to be modelled. An attractive tool to analyze these correlations is the method of direct numerical simulation. However, it is presently limited to small turbulence levels and simple geometries.

In a previous paper (Wörner & Grötzbach, 1993c) we used results of direct numerical simulations of natural convection in air and liquid sodium to analyze all terms in the transport equation for the vertical turbulent heat flux $\overline{u_3' T'}$. In this paper we extend this study to the transport equation for turbulent temperature fluctuations $\overline{T'^2}/2$, which is solved in some turbulence models to determine the production term due to buoyancy forces, appearing in the $\overline{u_3' T'}$ -equation.

PHYSICAL AND NUMERICAL MODEL

Rayleigh-Bénard Convection

A simple physical model for investigation of heat transfer phenomena by natural convection is the Rayleigh-Bénard convection. It is given by an infinite fluid layer which is confined by two rigid horizontal isothermal walls. The lower one is heated and the upper one is cooled. The physical problem is characterized by two dimensionless numbers: The Rayleigh number

$$Ra = \frac{g \beta \Delta T_W H^3}{\nu \kappa} \quad (1)$$

and the Prandtl number

$$Pr = \frac{\nu}{\kappa} \quad (2)$$

(where g = gravity, β = volume expansion coefficient, ΔT_W = temperature difference of the walls, H = depth of the fluid layer, ν = kinematic viscosity, and κ = thermal diffusivity). A further dimensionless number is the Grashof number

$$Gr = \frac{Ra}{Pr}. \quad (3)$$

In this paper we discuss results of two simulations. In the first one, the fluid is air ($Pr = 0.71$) and $Ra = 630\,000$, while in the second simulation it is liquid sodium ($Pr = 0.006$) and a Rayleigh number of $Ra = 24\,000$ is considered. Thus Ra and Pr are clearly different in both cases. However, the Grashof number is similar and of magnitude 10^6 . Thus in both simulations the velocity field is clearly turbulent (Wörner & Grötzbach 1993a). In air, where $Pr \approx 1$, the temperature field shows similar scales as the velocity field. In contrast, in liquid sodium the temperature field is largely laminar, as it is still governed by the large thermal conductivity.

Simulation Method

The numerical results for turbulent Rayleigh-Bénard convection which will be discussed in this paper are achieved by the direct simulation method. This means that the full three-dimensional time-dependent conservation equations of mass, momentum, and energy are solved on grids which resolve the largest and smallest scales of turbulence. Thus no turbulence model is used and the simulations do not depend on any model coefficients.

The simulations are performed with the TURBIT code (Grötzbach, 1987). It is based on a finite volume method and allows for direct numerical simulation of turbulent flow and heat transfer in simple channel geometries. Assuming the validity of the Boussinesq approximation, the governing equations are solved in dimensionless form. For normalization the channel height H , velocity $u_o = (g\beta\Delta T_W H)^{1/2}$, time H/u_o , pressure ρu_o^2 and temperature difference ΔT_W are used. Spatial discretization is based on a staggered grid and second order central finite differences. Time integration of the momentum equation is performed by the explicit Euler-Leapfrog scheme, whereas for the energy equation the semi-implicit Leapfrog-Crank-Nicholson scheme is used.

The boundary conditions are periodic ones in both horizontal directions, whereas at the lower and upper wall the no slip condition and constant wall temperatures are specified. To reduce the computation time, the simulation of sodium was started from the final data of a previous simulation ($Ra = 12\,000$, $Pr = 0.006$) with the same spatial discretization. For the simulation of air, final results of a former simulation ($Pr = 0.71$, $Ra = 380\,000$) were interpolated to a finer grid and used as initial data. The parameters and grid data of both simulations are given in Table 1. For verification of the numerical results by experimental data, see Wörner & Grötzbach (1993a,b).

Table 1: Parameters and grid data of the simulations:

$X_{1,2}$ horizontal extension of channel in terms of H , $N_{1,2}$ number of mesh cells in horizontal direction (equidistantly spaced), N_3 number of mesh cells in vertical direction (non-equidistantly spaced)

Pr	Ra	Gr	$X_{1,2}$	$N_{1,2}$	N_3
0.71	630 000	$8.9 \cdot 10^5$	7.92	200	39
0.006	24 000	$4 \cdot 10^6$	8.0	250	39

NUMERICAL RESULTS

Averaging Procedure

During the simulation the full three-dimensional results for the three velocity components, pressure and temperature are stored on disk at certain time intervals. For statistical analysis, averages \bar{y} for a calculated variable y are formed over horizontal planes and these are averaged over several time steps (typically 10 to 30). Vertical profiles are thus obtained from this averaging procedure, where $x_3 = 0$ corresponds to the lower and $x_3 = 1$ to the upper wall. To get meaningful statistical data only results within the fully developed flow regime are used.

Mean Temperature And Temperature Variance

Before we consider the exact transport equation of turbulent temperature fluctuations, we give results for the mean temperature \bar{T} and $\overline{T'^2}/2$ itself. In air we find an isothermal core and thin thermal boundary layers, see Fig. 1. In sodium a roughly linear mean temperature profile is identified, indicating that the thermal boundary layers extend almost over the whole channel. The corresponding profiles of $\overline{T'^2}/2$ for both simulations are given in Fig. 2. For air we find in the central region of the channel a constant plateau and two sharp peaks at the edges of the thermal boundary layers. In sodium only one maximum at channel midwidth is observed.

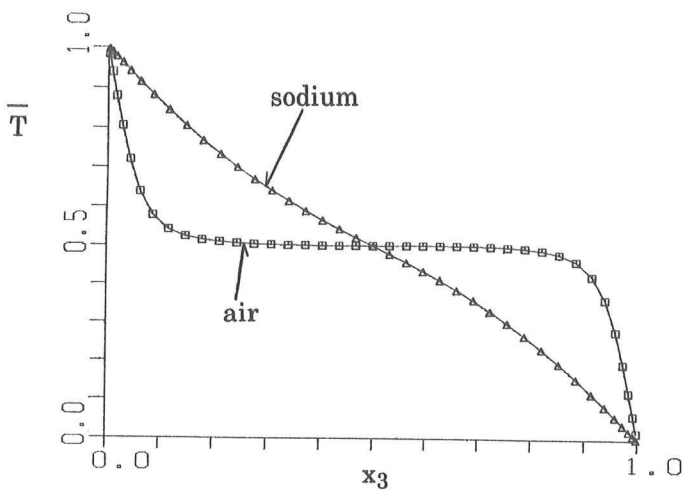


Fig. 1: Vertical mean temperature profile \bar{T} :
 (□) air, (Δ) sodium.

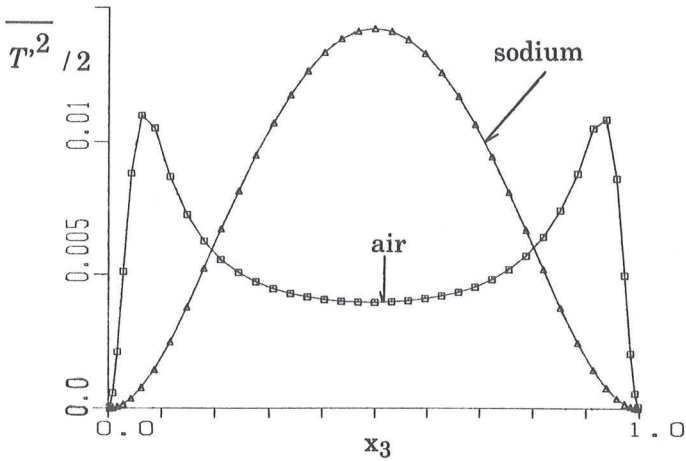


Fig. 2: Vertical profile of temperature variance $\overline{T'^2/2}$:
 (□) air, (Δ) sodium.

Balance Of Temperature Fluctuations $\overline{T'^2/2}$

In turbulent Rayleigh-Bénard convection, mean velocities averaged over long times are zero. Therefore, in the transport equation of turbulent temperature fluctuations, no convective transport exists. In fully developed flow, the exact equation for $\overline{T'^2/2}$ in dimensionless form reduces to

$$0 = \underbrace{-\frac{\partial}{\partial x_3} \left(\overline{u_3' T'^2/2} - \frac{1}{Pr\sqrt{Gr}} \frac{\partial \overline{T'^2/2}}{\partial x_3} \right)}_{D_g} - \underbrace{\overline{u_3' T'}}_{P_g} \frac{\partial \bar{T}}{\partial x_3} - \underbrace{\frac{1}{Pr\sqrt{Gr}} \frac{\partial \bar{T}}{\partial x_j} \frac{\partial \bar{T}}{\partial x_j}}_{\epsilon_g} \quad (4)$$

Here D_g denotes the diffusion of $\overline{T'^2/2}$. It consists of a turbulent and a molecular part. P_g is the production and ϵ_g the dissipation of $\overline{T'^2/2}$.

In Fig. 3 we show vertical profiles of the different terms for the simulation with air. The production term is zero at the walls, because the turbulent heat flux $\overline{u_3' T'}$ is zero, and in the isothermal core region because the mean temperature gradient vanishes. Thus P_g is non-zero only near the edges of the thermal boundary layers, where both the turbulent heat flux and the mean temperature gradient are finite. The sink term ϵ_g is almost constant in the centre of the channel and shows strong peaks near the walls. In the centre of the channel we observe the very unusual feature, that the dissipation ϵ_g is not balanced by the production term P_g , but rather by diffusion.

The balance of $\overline{T'^2/2}$ in sodium is quite different from that in air, see Fig. 4. In liquid sodium the gradient $\partial \bar{T}/\partial x_3$ is almost constant in the whole channel (see Fig. 1). In the core region the turbulent heat flux $\overline{u_3' T'}$ is constant too. Therefore the production term P_g shows a constant plateau in this region. As in the simulation with air, the diffusive transport of $\overline{T'^2/2}$ is of great importance.

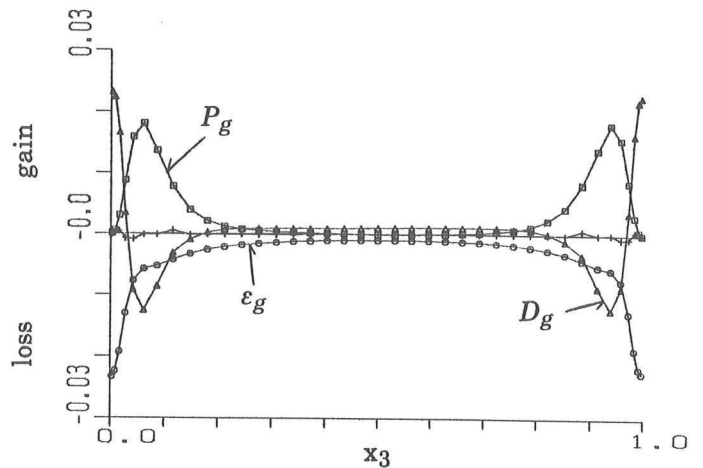


Fig. 3: Balance of the $\overline{T'^2/2}$ -equation for air, $Ra = 630\,000$.
 (□) P_g , (Δ) D_g , (○) ϵ_g , (+) balance difference.

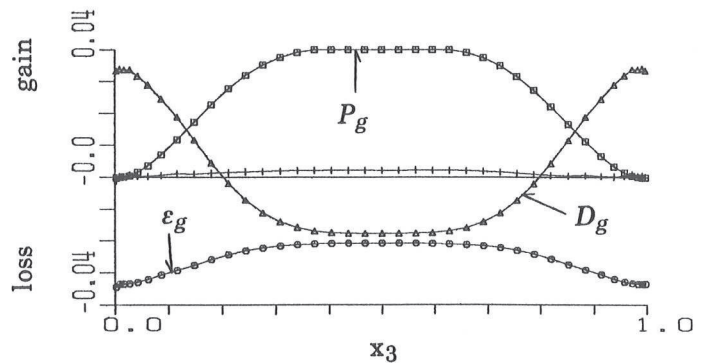


Fig. 4: Balance of the $\overline{T'^2/2}$ -equation for sodium, $Ra = 24000$.
 (□) P_g , (Δ) D_g , (○) ϵ_g , (+) balance difference.

Analysis Of Closure Assumptions Of Turbulence Models

Terms that have to be modelled in Eq. (4) in turbulence models are the triple correlation in the diffusion term (i.e. the turbulent diffusion) and the dissipation ε_g . In modelling the turbulent diffusion, gradient-type representations are usually chosen. The simple model of Spalding (1971) has the form

$$-\overline{u'_3 T'^2/2} = C'_T \frac{k^2}{\varepsilon} \frac{\partial(\overline{T'^2/2})}{\partial x_3}, \quad (5)$$

where k is the turbulence kinetic energy, ε the dissipation rate of k , and C'_T is a model coefficient. From our numerical results all terms in Eq. (5) can be directly evaluated. Therefore, we use the data base to determine the model coefficient C'_T . For both simulations the analyzed profile of C'_T shows strong peaks near the walls, Fig. 5. For air there is no region where C'_T takes a locally constant value of about 0.3, which is the recommended number for this coefficient. The singularity of C'_T in channel midwidth is a direct consequence of the gradient diffusion concept. As shown in Fig. 2, the gradient $\partial(\overline{T'^2/2})/\partial x_3$ is almost zero in the centre of the channel. Thus, according to model assumption (5), there should be nearly no diffusion in this region. The balance of $\overline{T'^2/2}$ in Fig. 3, however, shows that D_g is not zero, but has a finite value in the core region. The results for sodium are much smoother. As $\partial(\overline{T'^2/2})/\partial x_3$ is well defined (see Fig. 2) C'_T is almost constant. However, the analyzed value for C'_T is about 0.01 which is much smaller than that commonly used. The reason for this is that in liquid sodium, at the low Rayleigh number considered here, the temperature field is only weakly turbulent. Therefore in the diffusive transport of $\overline{T'^2/2}$, not the turbulent but rather the molecular part of D_g is dominant.

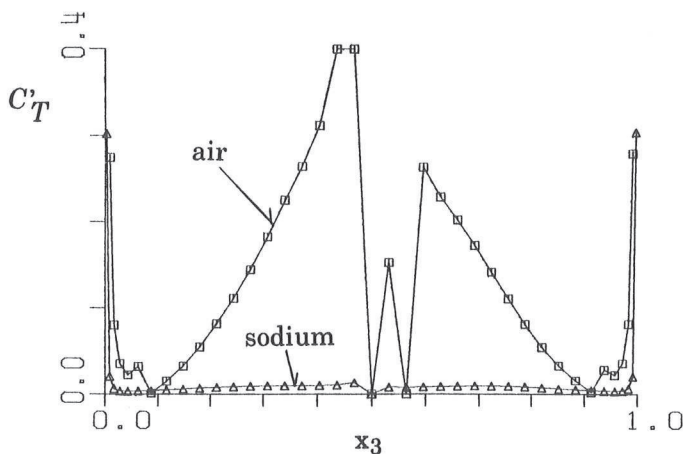


Fig. 5: Vertical profiles of the analyzed coefficient C'_T in the diffusion model (5). (\square) air, (Δ) sodium.

In some turbulent models a separate transport equation is solved to determine the sink term ε_g in Eq. (4). Rather simple models as that of Launder (1975) assume

$$\varepsilon_g = \frac{1}{R} \frac{\overline{T'^2/2}}{k} \varepsilon, \quad (6)$$

where ε_g is related to the turbulence kinetic energy and its dissipation rate. Here R is the ratio of the time scale characterizing the temperature fluctuations to that characterizing the velocity fluctuations, and this ratio is assumed to be constant in Launder's model. The vertical profile of R , analyzed from the numerical results, is given in Fig. 6. For air the value of R varies between 0.4 and 0.8 and thus agrees well with those commonly used in second moment closure models (Launder, 1976). However, R is not constant but shows strong vertical variations. The value of R for the simulation with sodium is much smaller than in the simulation with air. This indicates that the time scales of the velocity and temperature fields are quite different in liquid sodium and thus conventional values of R do not hold for low Rayleigh number convection in liquid metals. The present results, together with previous ones for liquid sodium at $Ra = 6000$ (Grötzbach & Wörner, 1992), suggest that R depends on both the Prandtl number and the turbulence level.

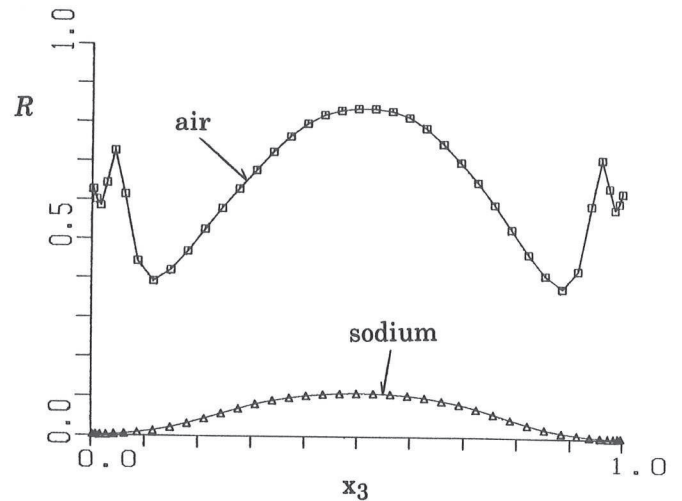


Fig. 6: Vertical profiles of the analyzed time scale ratio R in the ε_g -model (6). (\square) air, (Δ) sodium.

CONCLUSIONS

Based on direct numerical simulation results of turbulent Rayleigh-Bénard convection, an analysis of statistical features of temperature fluctuations in natural convection has been performed. Two simulations have been considered, one with air, showing a highly turbulent temperature field, and one with liquid sodium, where the temperature field is largely laminar. In both cases the maximum amplitude of temperature fluctuations occurs at the edges of the thermal boundary layers. In the case of air, this is the only region where the production term in the $\overline{T'^2/2}$ -equation is non-zero. The diffusive transport of $\overline{T'^2/2}$ is found to be of great importance. Both near the wall and in the core region, where the production term is zero, there is a balance between the diffusion and dissipation terms. Thus it is essential that models are used for D_g and ε_g which allow the reproduction of this special physical behaviour. The analysis of commonly used closure concepts has shown that these models are not able to predict correctly the unusual statistical properties of temperature fluctuations in natural convection. Our results show, that there is a strong need for a reliable diffusion model, which is not based on a gradient assumption.

NOMENCLATURE

C'_T	model coefficient
D_g	diffusion term in the $\overline{T'^2/2}$ -equation
g	gravity
Gr	Grashof number
H	depth of the fluid layer
k	turbulent kinetic energy
N_i	number of mesh cells
P_g	production term in the $\overline{T'^2/2}$ -equation
Pr	Prandtl number
R	time scale ratio
Ra	Rayleigh number
\overline{T}	mean temperature
$\overline{T'^2/2}$	temperature variance

ΔT_W	temperature difference between walls
u_o	velocity used for normalization
$\overline{u_i'T'}$	turbulent heat fluxes
$\overline{u_i'u_j'}$	Reynolds stresses
x_i	cartesian coordinates ($i=1,2$: horizontal, $i=3$: vertical)
$X_{1,2}$	horizontal extensions of the channel
β	volume expansion coefficient
ε	dissipation rate of turbulent kinetic energy
ε_g	sink term in the $\overline{T'^2/2}$ -equation
ν	kinematic viscosity
κ	thermal diffusivity
ρ	density

REFERENCES

- GRÖTZBACH, G., 1987. Direct numerical and large eddy simulation of turbulent channel flows. In: *Encyclopaedia of Fluid Mechanics*. Vol. 6, 1337-1391, Ed.: N.P. Chermisinoff, Gulf Publ. Houston.
- GRÖTZBACH, G., 1994. Direct numerical and large eddy simulation of turbulent heat transfer. This conference.
- GRÖTZBACH, G. & WÖRNER, M., 1992. Analysis of second order transport equations by numerical simulations of turbulent convection in liquid metals. *5th Topical Meeting on Nuclear Reactor Thermal Hydraulics (NURETH-5)*, Salt Lake City, USA, Vol. 2, 358-365.
- LAUNDER, B.E., 1975. On the effects of a gravitational field on the turbulent transport of heat and momentum. *J. Fluid Mech.* **67**, 569-581.
- LAUNDER, B.E., 1976. Heat and Mass Transport. In: *Topics in Applied Physics* **12**, 231-287, Ed.: P. Bradshaw, Springer.
- PEETERS, T.W.J. & HENKES, R.A.W.M., 1992. The Reynolds-stress model of turbulence applied to the natural convection boundary layer along a heated vertical plate. *Int. J. Heat Mass Transfer* **35**, 403-420.

RODI, W., 1980. *Turbulence models and their application in hydraulics - a state of the art review*. IAHR-publication, Delft.

SPALDING, D.B., 1971. Concentration fluctuations in a round turbulent free jet. *Chem. Eng. Sci.* **26**, 95-107.

WÖRNER, M. & GRÖTZBACH, G., 1993a. Contributions to turbulence modelling of natural convection in liquid metals by direct numerical simulation. *Joint Int. Conf. on Mathematical Methods and Supercomputing in Nuclear Applications*, Karlsruhe, Germany, Vol. 1, 224-235.

WÖRNER, M. & GRÖTZBACH, G., 1993b. Analysis of diffusion of turbulent kinetic energy by numerical simulations of natural convection in liquid metals. *6th Int. Topical Meeting on Nuclear Reactor Thermal Hydraulics (NURETH-6)*, Grenoble, France, Vol. 1, 186-193.

WÖRNER, M. & GRÖTZBACH, G., 1993c. Turbulent heat flux balance for natural convection in air and sodium analysed by direct numerical simulations. *5th Int. Symposium on Refined Flow Modelling and Turbulence Measurements*, Paris, France, 335-342.